

# Copper(I) Cuboctahedral Coordination Cages: Host–Guest Dependent Redox Activity\*\*

Qi-Ting He, Xiang-Ping Li, Yu Liu, Zhi-Quan Yu, Wei Wang, and Cheng-Yong Su\*

The self-assembly of coordination cages containing internal cavities with well-defined shape and size has achieved increasing prominence not only because of their aesthetic discrete structures, but also owing to their promising functionalities as metalated containers for storage, recognition, delivery, catalysis, or as molecular reactors.<sup>[1]</sup> Recent advances have revealed that enantioselective guest binding or stabilization of coordinatively unsaturated metal complexes can be accomplished by coordination cages,<sup>[2]</sup> and an unusual regioselective Diels–Alder reaction could be facilitated by coordination hosts.<sup>[3]</sup> These results may further inspire chemists to design and synthesize effective self-assembled container molecules capable of activating reactivity relying on the host–guest chemistry.

So far, the construction of coordination cages has mainly involved partially blocked metal ions such as Pd<sup>2+</sup> and Pt<sup>2+</sup> or “naked” metal ions of high coordination number (4 or 6).<sup>[4]</sup> Cage structures are less common for the low-coordination-number Ag<sup>+</sup>, Au<sup>+</sup>, and Cu<sup>+</sup> ions, which can afford the unique trigonal coordination mode not accessible to other metal ions.<sup>[5]</sup> Particularly, the Cu<sup>+</sup> ion is rarely used in the cage structure assembly,<sup>[6]</sup> probably because of its redox instability at ambient atmosphere. Nevertheless, incorporation of the redox-robust Cu<sup>+</sup> ion may be able to install reactive sites into the host molecules, or to activate reactivity of the substrate molecules, which is essential to an effective molecular reactor. It has been known that many Cu-containing enzymes perform a variety of critical biological functions, and their synthetic models for C–H bond activation has long been an important research objective.<sup>[7]</sup> Herein, we report the assembly of a series of Cu<sup>+</sup> cuboctahedral coordination cages by using a bulky triangular ligand and different Cu<sup>+</sup> salts, which show redox stability relying on counteranions and reactivity

towards arene C–H bond activation depending on the host–guest adaptability.

The triangular tris-monodentate ligand possessing three rotatable benzimidazole (Bim) arms, 1,3,5-tris(1-benzylbenzimidazol-2-yl)benzene (L), was prepared by substitution of 1,3,5-tris(2-benzimidazolyl)benzene. As depicted in Scheme 1, reaction of L with Cu<sup>+</sup> ion at room temperature readily resulted in formation of cage structure {guest[Cu<sup>I</sup><sub>4</sub>L<sub>4</sub>]·X·solvent} (guest = ClO<sub>4</sub><sup>−</sup>, X = 3 ClO<sub>4</sub><sup>−</sup>, **1a**; guest = I<sup>−</sup>, X = 3 I<sup>−</sup>, **2a**; guest = MeOH, X = 4 CF<sub>3</sub>SO<sub>3</sub><sup>−</sup>, **3a**, and X = 4 MeC<sub>6</sub>H<sub>4</sub>SO<sub>3</sub><sup>−</sup>, **4a**). For **1–2a**, Cu<sup>+</sup> salts were used, whereas for **3–4a** the Cu<sup>+</sup> ion originated from rapid in situ reduction of Cu<sup>2+</sup> (see below).<sup>[8]</sup> Interestingly, the Cu<sup>+</sup> complexes **3–4a** can be slowly oxidized to Cu<sup>2+</sup> complexes within several days with concomitant hydroxylation of L to 2,4,6-tris(1-benzylbenzimidazol-2-yl)phenol (LOH) at ambient temperature, giving the dinuclear complex [Cu<sup>II</sup><sub>2</sub>(LO)<sub>2</sub>(CF<sub>3</sub>SO<sub>3</sub>)<sub>2</sub>]<sup>−</sup>(CF<sub>3</sub>SO<sub>3</sub>)<sub>2</sub>·solvent (**3b**) and the tetranuclear complex [Cu<sup>II</sup><sub>4</sub>(LO)<sub>2</sub>(H<sub>2</sub>O)<sub>2</sub>(MeC<sub>6</sub>H<sub>4</sub>SO<sub>3</sub>)<sub>4</sub>] (**4b**). In contrast, Cu<sup>+</sup> complexes **1–2a** are relatively stable, remaining unchanged when kept in the mother liquor for several months. All complexes were unambiguously characterized by single-crystal X-ray diffraction. Detailed syntheses and characterization by elemental analysis, IR spectroscopy, <sup>1</sup>H NMR spectroscopy, and electrospray ionization mass spectrometry (ESIMS) are described in the Supporting Information.

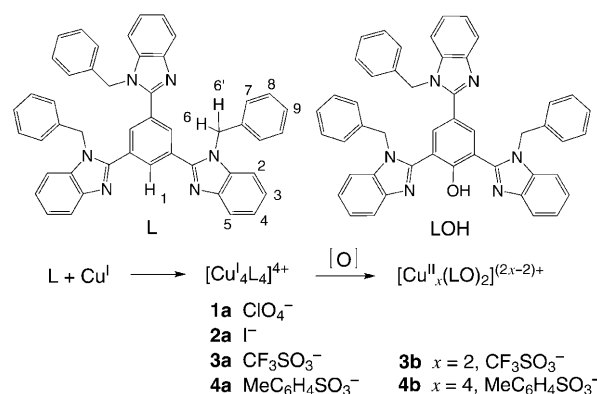
The X-ray crystal analyses confirmed the formation of the same M<sub>4</sub>L<sub>4</sub> coordination cage structure in all complexes **1–4a**, which have distinct counteranions of varied shapes and sizes (spherical ClO<sub>4</sub><sup>−</sup> and I<sup>−</sup>, linear CF<sub>3</sub>SO<sub>3</sub><sup>−</sup>, or planar MeC<sub>6</sub>H<sub>4</sub>SO<sub>3</sub><sup>−</sup>). Solvent molecules such as H<sub>2</sub>O and MeOH are present in the crystal lattice depending on the reaction

[\*] Q.-T. He, X.-P. Li, Y. Liu, Z.-Q. Yu, Prof. C.-Y. Su  
MOE Laboratory of Bioinorganic and Synthetic Chemistry  
State Key Laboratory of Optoelectronic Materials and Technologies  
School of Chemistry & Chemical Engineering  
Sun Yat-Sen University, Guangzhou 510275 (China)  
Fax: (+86) 20-8411-5178  
E-mail: cecssy@mail.sysu.edu.cn  
Homepage: <http://ce.sysu.edu.cn/scy/>

Prof. W. Wang  
State Key Laboratory of Applied Organic Chemistry  
Lanzhou University, Lanzhou 730000 (China)

[\*\*] This work was supported by the NSFC for Distinguished Young Scholars (20525310) and Innovative Groups (20821001), 973 Program of China (2007CB815302), the NSFC Projects (20673147, 20773167, 20731005) and RFDP of Higher Education.

Supporting information for this article is available on the WWW under <http://dx.doi.org/10.1002/anie.200902276>.



**Scheme 1.** Molecular structures of the ligand L and its hydroxylated product LOH, as well as the reaction routes for synthesis of the complexes.

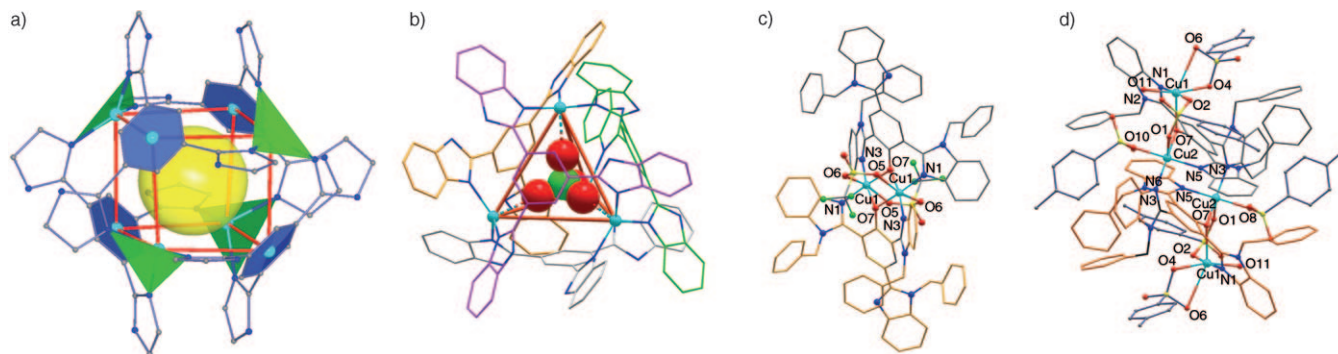


**Figure 1.** a) Representation of the  $[\text{Cu}_4\text{L}_4]^{4+}$  cages in **1–4a** showing a rectified cube. Benzyl groups and hydrogen atoms are omitted for clarity. The internal cavity is indicated by a yellow ball and rectification is demonstrated by trigonal  $\text{Cu}^+$  coordination plane and central benzene plane. b) Crystal structure of **1a** showing tetrahedral arrangement of  $\text{Cu}^+$  ions and  $\text{ClO}_4^-$  guest anion as a space-filling model. c) Crystal structure of **3b**. d) Crystal structure of **4b**.

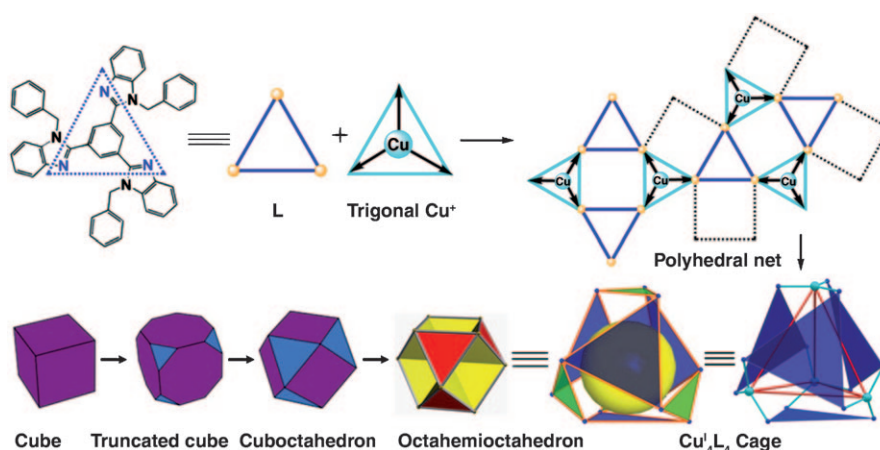
and crystallization conditions. As shown in Figures 1 and S1 (in the Supporting Information), the common  $[\text{Cu}_4\text{L}_4]^{4+}$  cage motif in **1–4a** consists of four  $\text{Cu}^+$  ions and four L ligands. Each  $\text{Cu}^+$  ion adopts trigonal coordination geometry to link three L ligands, whereas each L ligand takes on a propeller conformation in which the three Bim rings are twisted relative to the central benzene ring to connect three  $\text{Cu}^+$  ions. The Cu–N bond lengths fall in the range 1.977(7)–2.049(4) Å and the  $\angle\text{N–Cu–N}$  angles vary from 103.05(14) to 124.2(3)°. In general, the four  $\text{Cu}^+$  ions are arranged in a tetrahedral geometry with four ligands positioned parallel to the four faces of the  $\text{Cu}_4$  tetrahedron (Figure 1b, Figure S1c). Since every  $\text{Cu}^+$  ion is surrounded by three skewed Bim rings to form a trigonal  $\text{CuN}_3$  plane (Figure 1a,b), the internal cavity of  $[\text{Cu}_4\text{L}_4]^{4+}$  cage may be considered to be enclosed by four  $\text{CuN}_3$  planes and four central benzene planes, which constitute an aromatic core with twelve Bim rings fixed in pairs in six windows and twelve benzyl groups wrapping around (Figure S1b,d). The size of the cavity may be estimated by filling with a ball of 7 Å diameter.

A general description of such an  $\text{M}_4\text{L}_4$  cage is to consider it a truncated tetrahedron with trigonal  $\text{Cu}^+$  centers at the apices and triangular L ligands at the faces.<sup>[4]</sup> However, because the cage actually has six windows, a better description of the shape of the  $[\text{Cu}_4\text{L}_4]^{4+}$  cage cavity is to consider the middle points of the four central benzene rings and the four  $\text{Cu}^+$  centers as vertices, which gives a cube as shown in Figure 1a. Thus, the cavity of the  $[\text{Cu}_4\text{L}_4]^{4+}$  cage becomes a twisted cuboctahedron,<sup>[9]</sup> which is represented by a rectified cube with the eight corners truncated (Figure S1a). In this way, the resulting cuboctahedron can be described as consisting of eight triangles with six square windows open, so the cavity shape may also be regarded as an octahemioctahedron.<sup>[10]</sup>

The above analyses of the  $[\text{Cu}_4\text{L}_4]^{4+}$  cage, summarized in Scheme 2, may offer insight into its

assembly process. As suggested by Fujita and Stang,<sup>[11]</sup> molecular paneling or face-directed self-assembly by coordination often leads to formation of the highest symmetry polyhedron. In our cases, the L ligand features a rigid triangular  $\text{N}_3$  plane, and the trigonal  $\text{Cu}^+$  ion provides another kind of  $\text{CuN}_3$  triangular face. Connection through Cu–N bonding results in the assembly of four  $\text{N}_3$  and four  $\text{CuN}_3$  triangles (demonstrated by the polyhedral net depicted in Scheme 2), which can converge to form the most symmetric cuboctahedron with all triangles occupied by L and  $\text{Cu}^+$ . Until now, only a handful of cuboctahedral coordination cages have been reported, and these mainly focus on the use of  $[\text{M}_2(\text{CO}_2)_4]$  paddle-wheel building blocks,<sup>[9a,b]</sup> as well as a few  $\text{M}^{2+}$  complexes assembled from multidentate tripodal ligands.<sup>[9c,d]</sup>

Besides the entropy contribution arising from the highly symmetric assembly, one possible driving force in the formation of the  $[\text{Cu}_4\text{L}_4]^{4+}$  cage in **1–4a** may be the exact geometric match between the four triangular L ligands and the four trigonal  $\text{Cu}^+$  ions, which are able to align twelve Bim rings in six parallel pairs to form offset intramolecular  $\pi$ – $\pi$  interactions (Figure S1d). The template effect from anions may not play a major role because, although in **1–2a** the spherical  $\text{ClO}_4^-$  and  $\text{I}^-$  anions are hosted inside cages, the



**Scheme 2.** Assembly process of the  $[\text{Cu}_4\text{L}_4]^{4+}$  cages in **1–4a** showing the relationship of the cavity shape as cuboctahedron or octahemioctahedron, which can be formed from a truncated cube, and flat paper model indicating the connectivity between trigonal  $\text{Cu}^+$  ions and triangular ligands.

linear  $\text{CF}_3\text{SO}_3^-$  in **3a** and planar  $\text{MeC}_6\text{H}_4\text{SO}_3^-$  in **4a** are obviously mismatched with the cage cavity. Instead, MeOH molecules are encapsulated as guests (Figure S1c). In addition, the strong tendency to form  $\text{Cu}^+$  cage is evident from observations that **1a**, **3a**, and **4a** can be obtained directly from  $\text{Cu}^{2+}$  salts under ambient conditions, regardless of the anion. Our preliminary investigations into these reactions in MeOH by monitoring in situ through ESIMS spectra revealed that the cage assembly proceeded rapidly (within 10 minutes), which is indicative of fast  $\text{Cu}^{2+}$  to  $\text{Cu}^+$  reduction,<sup>[8]</sup> probably along with oxidation of MeOH to formaldehyde. The noticeable tendency towards cage formation may significantly affect the redox potential of the  $\text{Cu}^{2+}/\text{Cu}^+$  couple.

$^1\text{H}$  NMR and ESIMS measurements were carried out to elucidate the solution structures of the cage compounds. As shown in Figures 2, S2, and S3, the proton signals of L in **1a** were drastically shifted relative to those in the free ligand. Generally, the peaks of Bim H atoms (other than H5) are moved downfield, whereas the peaks of benzene, benzyl, and methylene H atoms are moved upfield. The assignments of these peaks have been verified carefully by  $^1\text{H}$ -COSY spectra with clear proton correlation (Figure S3). Analyses of these proton shifts show good consistency with the solid-state cage structure. Coordination of Bim groups to the  $\text{Cu}^+$  ions is expected to cause downfield shift of Bim protons owing to metal-induced effects.<sup>[5b]</sup> However, an abnormal upfield shift of the H5 peak is observed, as a result of specific disposition of the Bim rings upon formation of the cage structure. As discussed above, four  $\text{Cu}^+$  ions fix four benzene rings into an aromatic core with six Bim pairs arraying in an offset parallel fashion at cage windows. This configuration makes H5 atom point to an adjacent Bim ring, thus subjecting it to ring current shielding. Similarly, the H1 atom on the benzene ring is also directed towards a neighboring Bim ring, and is consequently upfield shifted. The H7–H9 atoms on the benzyl groups are all located above the central aromatic core, thereby displaying an upfield shift owing to arene ring shielding. The most informative change is observed for the H6 atoms on methylene group, which acts as a juncture to link Bim and benzyl groups. The singlet peak in free L is divided into two separate peaks with an upfield shift of more than 1.3 ppm. On the basis of the solid-state cage structure, two H6 atoms of each methylene are anchored beside a Bim ring and a central benzene ring in every six offset parallel Bim pairs. Because

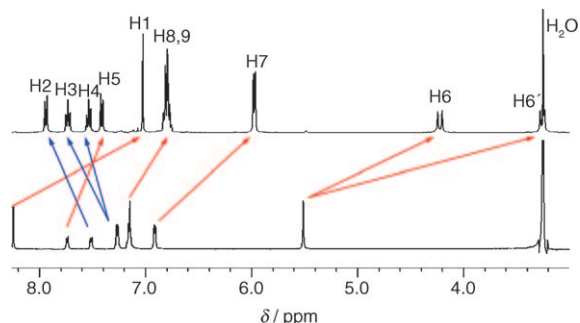


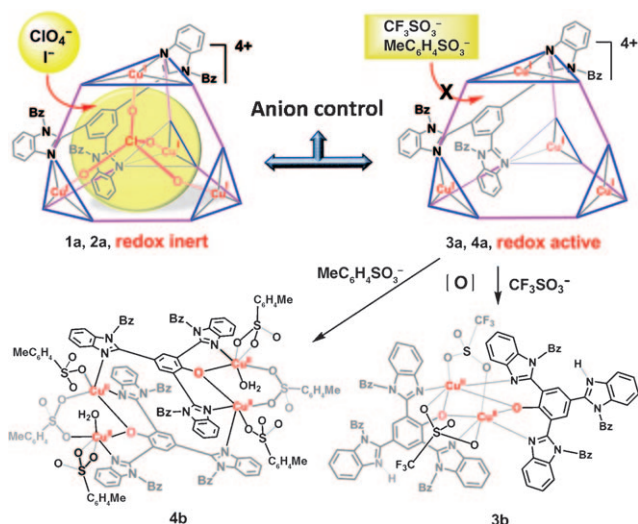
**Figure 2.**  $^1\text{H}$  NMR spectra of ligand L (bottom) and complex **1a** (top) measured in  $[\text{D}_6]\text{DMSO}$ . Shifts of the proton peaks are shown by the arrows.

the rigid cage structure does not allow the benzyl ring to rotate freely along the  $\text{N}-\text{C}_{\text{methylene}}$  bond, the two H6 atoms thus become diastereotopic, split into two resolved peaks, and move significantly upfield. These results suggest that the  $[\text{Cu}^1_4\text{L}_4]^{4+}$  cage structure is retained in solution; the spectra show only one set of well resolved signals in accordance with formation of a high symmetrical cuboctahedral structure. Further evidence for the solution structure came from the ESIMS spectra (Figures S4 and 5). The peaks related to the  $\text{M}_4\text{L}_4$  cage were observed and confirmed by comparisons between their measured and simulated isotopic distributions.

These  $\text{Cu}^+$  cages display distinct redox behavior in air depending on the nature of the anion. When crystals of the  $\text{Cu}^+$  complexes were kept in the mother liquors, slow conversion into  $\text{Cu}^{2+}$  complexes occurred, which can be easily judged from observation that the yellow crystals disappeared gradually and green crystals grew. Conversion of **3a** and **4a** into **3b** and **4b**, respectively, is complete within one week, but complexes **1a** and **2a** are stable in solution for several months. The structural analyses revealed a dinuclear structure for **3b** in which two  $\text{Cu}^{2+}$  ions take octahedral geometry (Figure 1c). Complex **4b** shows a tetranuclear structure containing two octahedral and two square-pyramidal  $\text{Cu}^{2+}$  ions (Figure 1d). In both structures, the ligand L was hydroxylated to LOH and acts as a bridging ligand to chelate two  $\text{Cu}^{2+}$  ions with the remaining coordination sites occupied by O atoms from  $\text{CF}_3\text{SO}_3^-$  or  $\text{MeC}_6\text{H}_4\text{SO}_3^-$  anions. Further identification of L hydroxylation was accomplished by ESIMS measurements. As seen in Figure S6, all salient peaks of **3b** can be assigned to dimeric or monomeric species containing the  $\text{LO}^-$  ion, confirming the formation of LOH from L.

Although a detailed mechanism of the hydroxylation of L is still waiting for thorough investigation, an  $\text{O}_2$ -activated arene C–H bond oxidation process, which has been widely accepted in various synthetic copper model complexes,<sup>[7]</sup> may be expected. A lot of predesigned multinuclear  $\text{Cu}^+$  precursors have been proven to be able to capture  $\text{O}_2$  molecules to mediate ligand hydroxylation, and the trigonal  $\text{Cu}^+$  ion in multinuclear enzymes is believed to be purposeful for  $\text{O}_2$  reactivity.<sup>[7]</sup> To investigate the role of the  $\text{Cu}^+$  cages in hydroxylation of L, we carried out a series of comparative experiments by treating L with different  $\text{Cu}^+$  and  $\text{Cu}^{2+}$  salts in MeOH at room temperature. In situ monitoring of the reaction medium with ESIMS spectra revealed that, regardless of whether  $\text{Cu}^+$  and  $\text{Cu}^{2+}$  salts were used, the  $[\text{Cu}^1_4\text{L}_4]^{4+}$  cage structures were formed quickly (within 10 minutes), but the hydroxylated LOH ligand could not be detected within 24 h. This result probably means that the  $\text{Cu}^+$  cage is the most favorable thermodynamic product in the reaction of L with  $\text{Cu}^+/\text{Cu}^{2+}$  salts, and hydroxylation of L is initiated later by  $\text{O}_2$  attack of the  $[\text{Cu}^1_4\text{L}_4]^{4+}$  cage. Once  $\text{Cu}^+$  ions capture  $\text{O}_2$  with conversion into  $\text{Cu}^{2+}$ , the cage could undergo structural rearrangement to facilitate the final hydroxylation of L. Such a process may also account for the formation of the final dinuclear and tetranuclear  $\text{Cu}^{2+}$  complexes **3b** and **4b**. Further investigations on the mechanical details of the hydroxylation are currently in progress.

On the basis of above discussions, host–guest dependent redox activity for coordination cages **1–4a** may be speculated,



**Scheme 3.** Schematic representation of the  $[\text{Cu}_4\text{L}_4]^{4+}$  cages showing that anions control the redox activity of the host molecules. Hydroxylation of the ligand **L** and formation of  $\text{Cu}^{2+}$  complexes **3b** and **4b** is shown.

as illustrated in Scheme 3. The cages **1–2a** can be considered redox inert, whereas cages **3–4a** are redox active. The cages **1–2a** host spherical  $\text{ClO}_4^-$  and  $\text{I}^-$  anions, whereas cages **3–4a** accommodate an MeOH guest with host–guest mismatched  $\text{CF}_3\text{SO}_3^-$  and  $\text{MeC}_6\text{H}_4\text{SO}_3^-$  anions lying outside the cage. The  $\text{ClO}_4^-$  ion in **1a** exactly matches the cavity with the four O atoms interacting with the four  $\text{Cu}_4$  ions ( $\text{Cu}\cdots\text{O}$ , 2.38 Å). In **2a**, the  $\text{I}^-$  guest forms  $\text{Cu}\cdots\text{I}$  interactions (2.91 Å) with two  $\text{Cu}^+$  ions. In contrast, in **3a** only one  $\text{Cu}^+$  ion interacts with the MeOH guest ( $\text{Cu}\cdots\text{O}$ , 2.38 Å). The bulky spherical guests in **1–2a** display good adaptability to the cuboctahedral cavity, thereby stabilizing the cage and protecting the four  $\text{Cu}^+$  ions against  $\text{O}_2$  attack. In contrast, the MeOH guest in **3–4a** can only deactivate one  $\text{Cu}^+$  ion, leaving a partial cavity and three trigonal  $\text{Cu}^+$  ions free to catch an  $\text{O}_2$  molecule. This difference may be the intrinsic reason that the cages **1–2a** are redox inert but the cages **3–4a** are redox active. Because the guest encapsulation in cages **1–4a** is determined by the shape and size of the counteranions, the host–guest redox dependence of the coordination cages may also be regarded as a control by the anions. One potential interest from this finding is that it might be possible to find a multi- $\text{Cu}^+$  structural model for C–H activation with reactivity under ambient conditions and redox activity that can be tuned through host–guest interactions.

In summary, a synthetically flexible but viable route to assemble  $\text{Cu}^+$  coordination cages has been achieved by the use of a triangular Bim-based bulky ligand **L**. The same  $[\text{Cu}_4\text{L}_4]^{4+}$  cages containing cuboctahedral cavity were obtained with counteranions of diverse shape and size. Redox dependence on the host–guest interaction is proposed for these cages, controllable through selection of the anions. Hydroxylation of the ligand under ambient conditions was observed from the structural conversion of the redox-active

cages. Although the intricate redox mechanism involved in these reactions remains largely unclear, we expect a follow-up study could offer an alternative way to explore catalytic functions by copper cage complexes.

Received: April 28, 2009  
 Published online: July 8, 2009

**Keywords:** cage compounds · copper · host–guest systems · redox activity · self-assembly

- [1] a) D. Fiedler, D. H. Leung, R. G. Bergman, K. N. Raymond, *Acc. Chem. Res.* **2005**, *38*, 351–360; b) R. W. Saalfrank, E. Uller, B. Demleitner, I. Bernt, *Struct. Bonding (Berlin)* **2000**, *96*, 149–175; c) F. Hof, J. Rebek, Jr., *Proc. Natl. Acad. Sci. USA* **2002**, *99*, 4775–4777; d) M. Yoshizawa, J. K. Klosterman, M. Fujita, *Angew. Chem.* **2009**, *121*, 3470–3490; *Angew. Chem. Int. Ed.* **2009**, *48*, 3418–3438.
- [2] a) D. Fiedler, D. H. Leung, R. G. Bergman, K. N. Raymond, *J. Am. Chem. Soc.* **2004**, *126*, 3674–3675; b) M. Kawano, Y. Kobayashi, T. Ozeki, M. Fujita, *J. Am. Chem. Soc.* **2006**, *128*, 6558–6559.
- [3] M. Yoshizawa, M. Tamura, M. Fujita, *Science* **2006**, *312*, 251–254.
- [4] a) S. Leininger, B. Olenyuk, P. J. Stang, *Chem. Rev.* **2000**, *100*, 853–908; b) B. J. Holliday, C. A. Mirkin, *Angew. Chem.* **2001**, *113*, 2076–2097; *Angew. Chem. Int. Ed.* **2001**, *40*, 2022–2043; *Angew. Chem.* **2001**, *113*, 2076–2097; c) S. P. Argent, H. Adams, T. Riis-Johannessen, J. C. Jeffery, L. P. Harding, M. D. Ward, *J. Am. Chem. Soc.* **2006**, *128*, 72–73; d) R. W. Saalfrank, H. Maid, A. Scheurer, *Angew. Chem.* **2008**, *120*, 8924–8956; *Angew. Chem. Int. Ed.* **2008**, *47*, 8794–8824; e) I. M. Oppel (née Müller), K. Föcker, *Angew. Chem.* **2008**, *120*, 408–411; *Angew. Chem. Int. Ed.* **2008**, *47*, 402–405.
- [5] a) S. Hiraoka, T. Yi, M. Shiro, M. Shionoya, *J. Am. Chem. Soc.* **2002**, *124*, 14510–14511; b) C. J. Sumbly, M. J. Hardie, *Angew. Chem.* **2005**, *117*, 6553–6557; *Angew. Chem. Int. Ed.* **2005**, *44*, 6395–6399; *Angew. Chem.* **2005**, *117*, 6553–6557; c) V. J. Catalano, B. L. Bennett, H. M. Kar, *J. Am. Chem. Soc.* **1999**, *121*, 10235–10236.
- [6] a) P. N. W. Baxter, J.-M. Lehn, B. O. Kneisel, G. Baum, D. Fenske, *Chem. Eur. J.* **1999**, *5*, 113–120; b) O. V. Dolomanov, A. J. Blake, N. R. Champness, M. Schröder, C. Wilson, *Chem. Commun.* **2003**, 682–683; c) C.-Y. Su, Y.-P. Cai, C.-L. Chen, M. D. Smith, W. Kaim, H.-C. zur Loye, *J. Am. Chem. Soc.* **2003**, *125*, 8595–8613.
- [7] a) L. M. Mirica, X. Ottenwaelder, T. D. Stack, *Chem. Rev.* **2004**, *104*, 1013–1045; b) E. A. Lewis, W. B. Tolman, *Chem. Rev.* **2004**, *104*, 1047–1076; c) K. D. Karlin, M. S. Nasir, B. I. Cohen, R. W. Cruse, S. Kaderli, A. D. Zuberbühler, *J. Am. Chem. Soc.* **1994**, *116*, 1324–1336; d) L. Casella, M. Gullotti, G. Pallanza, L. Rigoni, *J. Am. Chem. Soc.* **1988**, *110*, 4221–4227.
- [8] a) X.-M. Chen, M. L. Tong, *Acc. Chem. Res.* **2007**, *40*, 162–170; b) J. Y. Lu, *Coord. Chem. Rev.* **2003**, *246*, 327–347.
- [9] a) Y. Ke, D. J. Collins, H.-C. Zhou, *Inorg. Chem.* **2005**, *44*, 4154–4156; b) B. F. Abrahams, S. J. Egan, R. Robson, *J. Am. Chem. Soc.* **1999**, *121*, 3535–3536.
- [10] J. Lu, A. Mondal, B. Moulton, M. J. Zaworotko, *Angew. Chem.* **2001**, *113*, 2171–2174; *Angew. Chem. Int. Ed.* **2001**, *40*, 2113–2116.
- [11] a) M. Fujita, K. Umamoto, M. Yoshizawa, N. Fujita, T. Kusukawa, K. Biradha, *Chem. Commun.* **2001**, 509–518; b) S. Russell, P. Stang, *Acc. Chem. Res.* **2002**, *35*, 972–983.